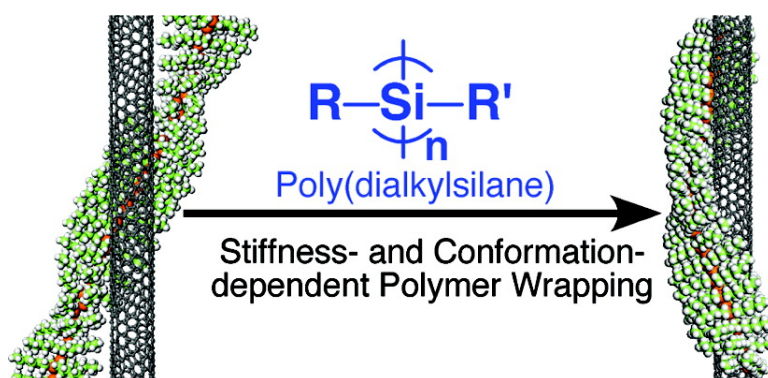


## Stiffness- and Conformation-Dependent Polymer Wrapping onto Single-Walled Carbon Nanotubes

Masanobu Naito, Kazuyuki Nobusawa, Hisanari Onouchi, Masashi Nakamura, Ken-ichiro Yasui, Atsushi Ikeda, and Michiya Fujiki

*J. Am. Chem. Soc.*, **2008**, 130 (49), 16697-16703 • DOI: 10.1021/ja806109z • Publication Date (Web): 17 November 2008

Downloaded from <http://pubs.acs.org> on February 8, 2009



### More About This Article

Additional resources and features associated with this article are available within the HTML version:

- Supporting Information
- Access to high resolution figures
- Links to articles and content related to this article
- Copyright permission to reproduce figures and/or text from this article

[View the Full Text HTML](#)

## Stiffness- and Conformation-Dependent Polymer Wrapping onto Single-Walled Carbon Nanotubes

Masanobu Naito,\* Kazuyuki Nobusawa, Hisanari Onouchi, Masashi Nakamura, Ken-ichiro Yasui, Atsushi Ikeda, and Michiya Fujiki

Graduate School of Materials Science, Nara Institute of Science and Technology,  
8916-5 Takayama, Ikoma, Nara 630-0192, Japan

Received August 4, 2008; E-mail: mnaito@ms.naist.jp

**Abstract:** This work reports the effect of stiffness and conformation of chain-like polymers on wrapping behaviors around single-walled carbon nanotubes (SWNT). As a model of chain-like polymers, three kinds of poly(dialkylsilane) (PSi)s with random-coiled, flexible, and semiflexible main chains were employed. Complexes of PSi and SWNT were prepared using mechanochemical high-speed vibration milling (HSVM). Stiffness-dependent polymer wrapping behaviors were investigated using combinational analyses with a differential scanning calorimeter, transmission electron microscopy, and atomic force microscopy. Furthermore, the conformational behaviors of the PSi's wrapped onto SWNTs were characterized spectroscopically with ordinary UV spectroscopy. Random-coiled and flexible PSi's were successfully wrapped onto small bundles of SWNTs, in which their conformations were changed to fit the surface curvatures of the SWNTs. However, semiflexible PSi could not form a complex with SWNTs, and its conformation remained unchanged even after the same HSVM process. Knowledge gained from this study may lead to a new approach to molecular design of chain-like polymers for efficient wrapping materials for SWNTs.

### Introduction

Single walled-carbon nanotubes (SWNT)s have attracted a great deal of attention due to their extraordinary electronic, mechanical, and optical properties.<sup>1–4</sup> However, their poor solubility and processability have hindered chemical manipulation and their further use in applications.<sup>5</sup> To overcome these disadvantages, much research on noncovalent wrapping around the surface of SWNTs with various chain-like polymers,<sup>6</sup> including DNAs,<sup>7,8</sup> carbohydrates,<sup>9,10</sup> peptides,<sup>11,12</sup> and  $\pi$ -con-

jugated polymers,<sup>13,14</sup> has been reported. When the polymer-wrapping techniques are applied for developing SWNT-based nanomaterials or nanodevices,<sup>15</sup> understanding the driving forces by which the chain-like polymers successfully wrap individual tubes and small bundles is essential. However, the driving forces in determining the polymer-wrapping of SWNTs are still debated. In general, it has been widely accepted that various noncovalent intermolecular interactions, such as  $\pi$ - $\pi$ ,<sup>12</sup> CH- $\pi$ ,<sup>16</sup> and van der Waals interactions,<sup>17,18</sup> play a significant role in promoting the helical wrapping of chain-like polymers around SWNTs. In contrast, recent computational studies suggested that helical wrapping is a general phenomenon at the interface between chain-like polymers and SWNTs, which is induced by both sufficient stiffness of the chain-like polymers and the highly curved surface of the SWNTs.<sup>19–21</sup> Here, it is particularly important that, in addition to the specific interactions between the polymer and SWNTs, such as  $\pi$ - $\pi$ , CH- $\pi$ , and van der Waals interactions, the stiffness and conformation of chain-like polymers may strongly contribute to wrapping behavior onto the cylindrical SWNT surface. These arguments, however, have been made solely on the basis of computational

- (1) Iijima, S. *Nature* **1991**, *354*, 56–58.
- (2) Baughman, R. H.; Zakhidov, A. A.; de Heer, W. A. *Science* **2002**, *297*, 787–792.
- (3) Ajayan, P. M. *Chem. Rev.* **1999**, *99*, 1787–1799.
- (4) Ajayan, P. M.; Zhou, O. Z. *In Carbon Nanotubes* **2001**, *80*, 391–425.
- (5) Thess, A.; Lee, R.; Nikolaev, P.; Dai, H. J.; Petit, P.; Robert, J.; Xu, C. H.; Lee, Y. H.; Kim, S. G.; Rinzler, A. G.; Colbert, D. T.; Scuseria, G. E.; Tomaneck, D.; Fischer, J. E.; Smalley, R. E. *Science* **1996**, *273*, 483–487.
- (6) Tasis, D.; Tagmatarchis, N.; Bianco, A.; Prato, M. *Chem. Rev.* **2006**, *106*, 1105–1136.
- (7) Zheng, M.; Jagota, A.; Semke, E. D.; Diner, B. A.; Mclean, R. S.; Lustig, S. R.; Richardson, R. E.; Tassi, N. G. *Nat. Mater.* **2003**, *2*, 338–342.
- (8) Nakashima, N.; Okuzono, S.; Murakami, H.; Nakai, T.; Yoshikawa, K. *Chem. Lett.* **2003**, *32*, 456–457.
- (9) Kim, O.-K.; Je, J. T.; Baldwin, J. W.; Kooi, S.; Pehrsson, P. E.; Buckley, L. J. *J. Am. Chem. Soc.* **2003**, *125*, 4426–4427.
- (10) Numata, M.; Asai, M.; Kaneko, K.; Bae, A.-H.; Hasegawa, T.; Sakurai, K.; Shinkai, S. *J. Am. Chem. Soc.* **2005**, *127*, 5875–5884.
- (11) Dieckmann, G. R.; Dalton, A. B.; Johnson, P. A.; Razal, J.; Chen, J.; Giordano, G. M.; Munoz, E.; Musselman, I. H.; Baughman, R. H.; Draper, R. K. *J. Am. Chem. Soc.* **2003**, *125*, 1770–1777.
- (12) Zorbas, V.; Ortiz-Acevedo, A.; Dalton, A. B.; Yoshida, M. M.; Dieckmann, G. R.; Draper, R. K.; Baughman, R. H.; Jose-Yacamán, M.; Musselman, I. H. *J. Am. Chem. Soc.* **2004**, *126*, 7222–7227.

- (13) Chen, J.; Liu, H. Y.; Weimer, W. A.; Halls, M. D.; Waldeck, D. H.; Walker, G. C. *J. Am. Chem. Soc.* **2002**, *124*, 9034–9035.
- (14) Nish, A.; Hwang, J.-Y.; Doig, J.; Nicholas, R. J. *Nat. Nanotechnol.* **2007**, *2*, 640–646.
- (15) Dai, H.-J. *Acc. Chem. Res.* **2002**, *35*, 1035–1044.
- (16) Baskaran, D.; Mays, J. W.; Bratcher, M. S. *Chem. Mater.* **2005**, *17*, 3389–3397.
- (17) Gao, H.-j.; Kong, Y. *Ann. Rev. Mater. Res.* **2004**, *34*, 123–150.
- (18) Xie, Y. H.; Soh, A. K. *Mater. Lett.* **2005**, *59*, 971–975.
- (19) Gurevitch, I.; Srebnik, S. *Chem. Phys. Lett.* **2007**, *444*, 96–100.
- (20) Kusner, I.; Srebnik, S. *Chem. Phys. Lett.* **2006**, *430*, 84–88.
- (21) Gurevitch, I.; Srebnik, S. *J. Chem. Phys.* **2008**, *128*, 144901.

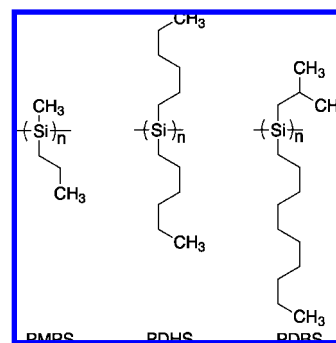
studies, due to the absence of both proper models of chain-like polymers whose main chain stiffness can be tailored by molecular design, and the absence of observation systems to monitor the subtle conformational changes in single layers on highly curved SWNT surfaces with ultrahigh sensitivity and accuracy in real-time.

In this work, we report, for the first time, the relationship between the stiffness of chain-like polymers and polymer-wrapping onto the SWNT surface, using combinational analyses with differential scanning calorimetry (DSC), transmission electron microscopy (TEM), and atomic force microscopy (AFM). Furthermore, the conformational behaviors of chain-like polymers wrapped on SWNTs were spectroscopically probed by means of ordinary UV spectroscopy.

## Results and Discussion

As a model of the chain-like polymers,  $\sigma$ -conjugated organic silicon nanowires, poly(dialkylsilane) (PSi), were employed, because their main chain stiffness, namely the persistent length ( $q$ ), can be tailored by the well-established molecular designs of their monomers, ranging from several to  $\sim 100$  nm,<sup>22,23</sup> and because both global and main chain conformations on the SWNT were easily estimated using ordinary UV spectroscopy, for the following reasons: the global conformations of chain-like polymers, such as rod-like, semiflexible, flexible, and random-coiled chains, can be conventionally classified by the viscosity index,  $\alpha$ ,<sup>24,25</sup> but measurement of the viscosity index requires complicated techniques and is limited to dilute solutions only. Alternatively, PSi's exhibit UV absorption bands around 300–380 nm, due to the  $\text{Si}\sigma\text{--Si}\sigma^*$  transition of the Si main chain.<sup>26,27</sup> Utilizing the characteristic UV absorption bands, a clear relationship among the main-chain peak intensities per silicon repeat unit,  $\epsilon$  (Si repeat unit)<sup>-1</sup>dm<sup>3</sup>cm<sup>-1</sup>,  $\alpha$ , and the full width at half-maximum (fwhm) has been established.<sup>22</sup> Thus, the value of  $\epsilon$  increases exponentially as a function of the value of  $\alpha$ , but the fwhm decreases. From this relationship, the global conformations can be easily estimated by the values of  $\epsilon$  and fwhm under various sets of conditions, even in bulk solid or thin films, as well as in solutions.<sup>28</sup> Furthermore, it is well-known that the maximum UV absorption wavelength ( $\lambda_{\text{max}}$ ) of the PSi's is closely connected to the main chain helical conformations. For example, when dialkyl substituted PSi's adopt the conformations of the deviant (dihedral angle,  $\phi$ :  $\sim 150^\circ$ ), transoid ( $\phi$ :  $\sim 165^\circ$ ), and anti ( $\phi$ :  $\sim 180^\circ$ ), the  $\lambda_{\text{max}}$  of the UV absorption bands appear at  $\sim 320$ , 355, and 370 nm, respectively.<sup>29–31</sup> Herein, we specifically chose three typical PSi's with markedly different  $\alpha$  values, poly(methyl-*n*-propylsilane) (PMPS) ( $M_w$ :  $1.4 \times 10^4$ , polydispersity index (PDI): 2.75, averaged molecular length ( $L$ ): 30.3 nm,  $\alpha$ : 0.46), poly(di-*n*-hexylsilane) (PDHS) ( $M_w$ :  $3.5 \times 10^4$ , PDI: 1.04,  $L$ : 32.6 nm,  $\alpha$ : 0.83), and poly(*n*-decyl-*i*-butylsilane) (PDBS) ( $M_w$ :  $6.8 \times$

**Scheme 1.** Poly(dialkylsilane)s Used in This Study<sup>a</sup>



<sup>a</sup> Poly(methyl-*n*-propylsilane) (PMPS) ( $M_w$ :  $1.4 \times 10^4$ , polydispersity index (PDI): 2.75, averaged molecular length ( $L$ ): 30.2 nm,  $\alpha$ : 0.46), poly(di-*n*-hexylsilane) (PDHS) ( $M_w$ :  $3.5 \times 10^4$ , PDI: 1.04,  $L$ : 32.6 nm,  $\alpha$ : 0.83), and poly(*n*-decyl-*i*-butylsilane) (PDBS) ( $M_w$ :  $6.8 \times 10^4$ , PDI: 1.03,  $L$ : 55.0 nm,  $\alpha$ : 1.18) were employed as models of random-coiled, flexible, and semiflexible chains, respectively.

$10^4$ , PDI: 1.03,  $L$ : 55.0 nm,  $\alpha$ : 1.18) as models of random-coiled, flexible, and semiflexible chains, respectively (Scheme 1 and Table S1 in Supporting Information).<sup>32</sup> Here, the values of  $L$  were given by 0.185 nm (value of the Si–Si projection length of PSi)  $\times n$ . Note that the difference in the values of  $L$  and PDI among PSi's are thought not to significantly affect wrapping behavior because the CoMoCAT-SWNTs are several tens of times longer than PSi's used in this study. The PSi's were prepared by a Wurtz-type condensation reaction of the corresponding dichlorosilane with sodium in toluene at 120 °C in the presence of 18-crown-6 ( $\sim 2$  mol% to the monomer), and then isolated by fractional precipitation with careful successive additions of 2-propanol, ethanol, and methanol.<sup>33,34</sup>

Recent progress in the preparation of SWNTs with high-performance catalysts can provide SWNTs with an almost uniform diameter and relatively narrow diameter distribution. In this study, SWNTs prepared by CoMoCAT method with an average diameter of 0.8 nm were employed because the CoMoCAT-SWNTs comprise more than 50% of two specific structures with (6,5) and (7,5) chiral vectors.<sup>35</sup> The CoMoCAT-SWNTs were purchased from South West Nano Technologies, Inc. (OK, USA), and were used without further purification.

From among various polymer-wrapping techniques,<sup>6,36</sup> we specifically chose high-speed vibration milling (HSVM) for efficient preparation of the complexes of PSi and SWNTs because HSVM can cause pristine SWNTs to mechanochemically debundle through complexation with only a solubilizing

- (22) Fujiki, M. *J. Am. Chem. Soc.* **1996**, *118*, 7424–7425.  
 (23) Fujiki, M. *Macromol. Rapid Commun.* **2001**, *22*, 539–563.  
 (24) Flory, P. J. *Principles of Polymer Chemistry*; Cornell University Press: Ithaca, NY, 1953.  
 (25) Tanford, C. *Physical Chemistry of Macromolecules*; John Wiley Press: New York, 1961.  
 (26) West, R. J. *Organomet. Chem.* **1986**, *300*, 327–346.  
 (27) Hallmark, V. M.; Sooriyakumaran, R.; Miller, R. D.; Rabolt, J. F. *J. Chem. Phys.* **1989**, *90*, 2486–2491.  
 (28) Naito, M.; Fujiki, M. *Soft Matter* **2008**, *4*, 211–223.  
 (29) Michl, J.; West, R. *Acc. Chem. Res.* **2000**, *33*, 821–823.  
 (30) West, R. J. *Organomet. Chem.* **2003**, *685*, 6–8.  
 (31) Tsuji, H.; Michl, J.; Tamao, K. *J. Organomet. Chem.* **2003**, *685*, 9–14.

- (32) The  $\alpha$  values were determined by an SEC with a Shimadzu model A-103 (Kyoto, Japan) (eluent: tetrahydrofuran; flow rate: 1.0 mL/min; and column temperature: 40 °C) equipped with a TSKgel GMHHR-M (Tosoh Bioscience, Japan) (300 mm in length, 7.8 mm in diameter), a Shimadzu RID-10A (Kyoto, Japan) refractive index detector, and a Viscotek model T60A triple detector (Houston, TX) consisting of a right-angle laser light scattering detector (RALLS) ( $\lambda_0$ : 670 nm) and a four-capillary differential viscometer. The results were analyzed using worm-like cylinder theory (Viscotek, built-in program).  
 (33) Miller, R. D.; Michl, J. *Chem. Rev.* **1989**, *89*, 1359–1410.  
 (34) Fujiki, M. *J. Am. Chem. Soc.* **1994**, *116*, 11976–11981.  
 (35) Bachilo, S. M.; Balzano, L.; Herrera, J. E.; Pompeo, F.; Resasco, D. E.; Weisman, R. B. *J. Am. Chem. Soc.* **2003**, *125*, 11186–11187.  
 (36) Grossiord, N.; Loos, J.; Regev, O.; Koning, C. E. *Chem. Mater.* **2006**, *18*, 1089–1099.

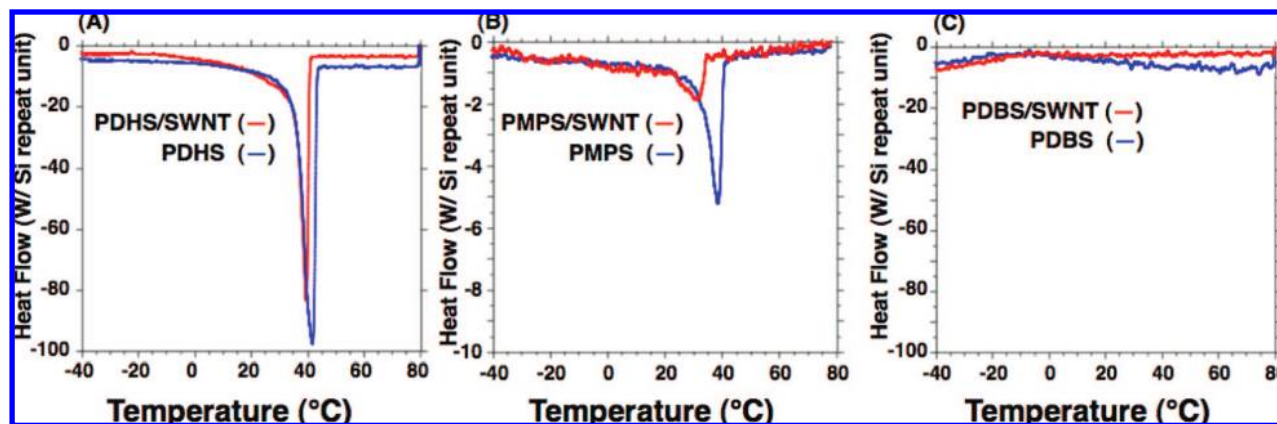


**Figure 1.** DSC thermograms of PSi and PSi/SWNT complexes. (A) PDHS (blue) and PDHS/SWNT (red), (B) PMPS (blue) and PMPS/SWNT (red), and (C) PDBS (blue) and PDBS/SWNT (red).

agent, and therefore without any organic/aqueous solvents.<sup>37–42</sup> Mixtures of pristine SWNTs (1.0 mg) and PSi's {15.0  $\mu\text{mol}$  (Si repeating unit)} were placed in an agate capsule together with two agate mixing balls. They were mixed vigorously at 1800 rpm for 20 min using a high-speed vibration mill (MM200, Retsch, Germany). The complexes of PSi and SWNTs (PSi/SWNT) obtained were dispersed in 10.0 mL of isooctane, and were then passed through a 0.5  $\mu\text{m}$  filter to eliminate the insoluble portions of the SWNT bundles. Using a size exclusion chromatography (SEC) measurement, it was confirmed that PSi's did not shear through the HSVM, because their molecular weights were unchanged before and after complexation.

First, to address the question of how the main chain stiffness of the PSi's affects complexation with SWNTs through the HSVM, DSC measurements of PSi's with various degrees of stiffness and the mixtures of PSi's and SWNTs (PSi/SWNT) were carried out. Figure 1 shows the DSC thermograms of PSi's and PSi/SWNT mixtures prepared by the HSVM. Flexible PDHS exhibited an intense endothermic peak ( $T_m$ ) at 41.9  $^{\circ}\text{C}$  with  $\Delta H$  of 3.3  $\text{kcal mol}^{-1}$  (Si repeating unit), which was in agreement with that in the literature [ $T_m$ : 41  $^{\circ}\text{C}$ ,  $\Delta H$ :  $\sim 4.0$   $\text{kcal mol}^{-1}$  (Si repeating unit)]<sup>43</sup> (blue line in Figure 1A). After the HSVM, the  $T_m$  peak shifted lower by 2.5  $^{\circ}\text{C}$  and the value of  $\Delta H$  slightly decreased to 2.7  $\text{kcal mol}^{-1}$  (Si repeating unit), (red line in Figure 1A). PMPS also showed an endothermic peak at 38.4  $^{\circ}\text{C}$ ,<sup>44</sup> which markedly shifted lower to 30.7  $^{\circ}\text{C}$ , and a greatly decreased  $\Delta H$  value which shifted from 0.19 to 0.05  $\text{kcal mol}^{-1}$  (Si repeating unit) after complexation with SWNTs (Figure 1B).<sup>45</sup> The endothermic peak of PMPS alone is also almost identical to that reported in the literature [ $T_m$ : 43.8  $^{\circ}\text{C}$ ,  $\Delta H$ : 0.23  $\text{kcal mol}^{-1}$  (Si repeating unit)].<sup>44</sup> Here, the endothermic

peaks at around 30–40  $^{\circ}\text{C}$ , as often seen in certain PSi's with symmetrical/asymmetrical alkyl side chains,<sup>26</sup> resulted from melting the closely packed alkyl side chains when the PSi's underwent a phase transition from a solid to a liquid crystalline mesophase. Therefore, the significant changes in endothermic peaks could be caused by disordering the crystallized alkyl side chains of PDHS or PMPS in the solid phases during complexation with SWNTs through the HSVM. However, neither PDBS nor PDBS/SWNT had an apparent endothermic peak between  $-40$  and  $80$   $^{\circ}\text{C}$ , indicating that the semiflexible PSi's did not undergo such phase transitions over the range of the operating temperatures (Figure 1C). Here, the DSC results led to the hypothesis that the key to successful complexation of PSi and SWNTs through HSVM may be the degree of the main chain stiffness of PSi's; that is, random-coiled PMPS or flexible PDHS could easily form complexes with SWNTs, whereas the semiflexible PDBS could not complex with SWNTs, even through the same HSVM procedure.

To obtain more reliable and direct evidence of the stiffness-dependent polymer wrapping on SWNTs, detailed structures of PSi/SWNT complexes prepared by HSVM were observed with a high-resolution TEM (JEM-31000FEF electron microscope at 300 kV, JEOL, Japan). The features observed obviously depended on the main chain stiffness of the PSi's. All samples were cast on a microgrid and then dried under a gentle stream of  $\text{N}_2$  gas. Figure 2 shows the TEM micrographs of PSi/SWNT complexes. In the PDHS/SWNT complex, fibrous structures with diameters in the range of 1–20 nm were observed (Figure 2A). These fibers appear to be the partially debundled SWNTs wrapped by PDHS. Similarly, in the PMPS/SWNT complex, we observed fibrous structures (Figure 2B). Judging from the average diameter of CoMoCAT-SWNT (0.8 nm), these fibrous structures with  $\sim 20$  nm in diameter consist of several SWNT single chains. Furthermore, from the enlarged TEM image of Figure 2B, we found that PMPS wrapped on the SWNTs in helical structures with both right and left handed helicities, reflecting the coexistence of the same amounts of *P*- and *M*-screw senses in the optically inactive PMPS (Figure 2B'). In contrast, PDBS/SWNT formed nanodomains with an area of approximately 10 nm by 10 nm, instead of the debundled SWNTs. The nanodomains consisted of highly oriented straight rods (Figure 2C). From an enlarged image of part C, the

(37) Nobusawa, K.; Ikeda, A.; Tanaka, Y.; Hashizume, M.; Kikuchi, J.-i.; Shirakawa, M.; Kitahara, T.; Fujita, N.; Shinkai, S. *Chem. Commun.* **2008**, 1801–1803.

(38) Nobusawa, K.; Ikeda, A.; Kikuchi, J.-i.; Kawano, S.-i.; Fujita, N.; Shinkai, S. *Angew. Chem., Int. Ed.* **2008**, *47*, 4577–4580.

(39) Ikeda, A.; Tanaka, Y.; Nobusawa, K.; Kikuchi, J.-i. *Langmuir* **2007**, *23*, 10913–10915.

(40) Ikeda, A.; Nobusawa, K.; Hamano, T.; Kikuchi, J.-i. *Org. Lett.* **2006**, *8*, 5489–5492.

(41) Ikeda, A.; Hamano, T.; Hayashi, K.; Kikuchi, J.-i. *Org. Lett.* **2006**, *8*, 1153–1156.

(42) Ikeda, A.; Hayashi, K.; Konishi, T.; Kikuchi, J.-i. *Chem. Commun.* **2004**, 1334–1335.

(43) Miller, R. D.; Hofer, D.; Rabolt, J.; Fickes, G. N. *J. Am. Chem. Soc.* **1985**, *107*, 2172–2174.

(44) Jambe, B.; Jonas, A.; Devaux, J. *J. Polym. Sci., Part B: Polym. Phys.* **1997**, *35*, 1533–1543.

(45)  $\Delta H$  values [ $\text{kcal mol}^{-1}$  (Si repeating unit)] of PDHS and PMPS were calculated using the previously reported data of 84  $\text{J g}^{-1}$  and 19  $\text{J g}^{-1}$ , respectively.

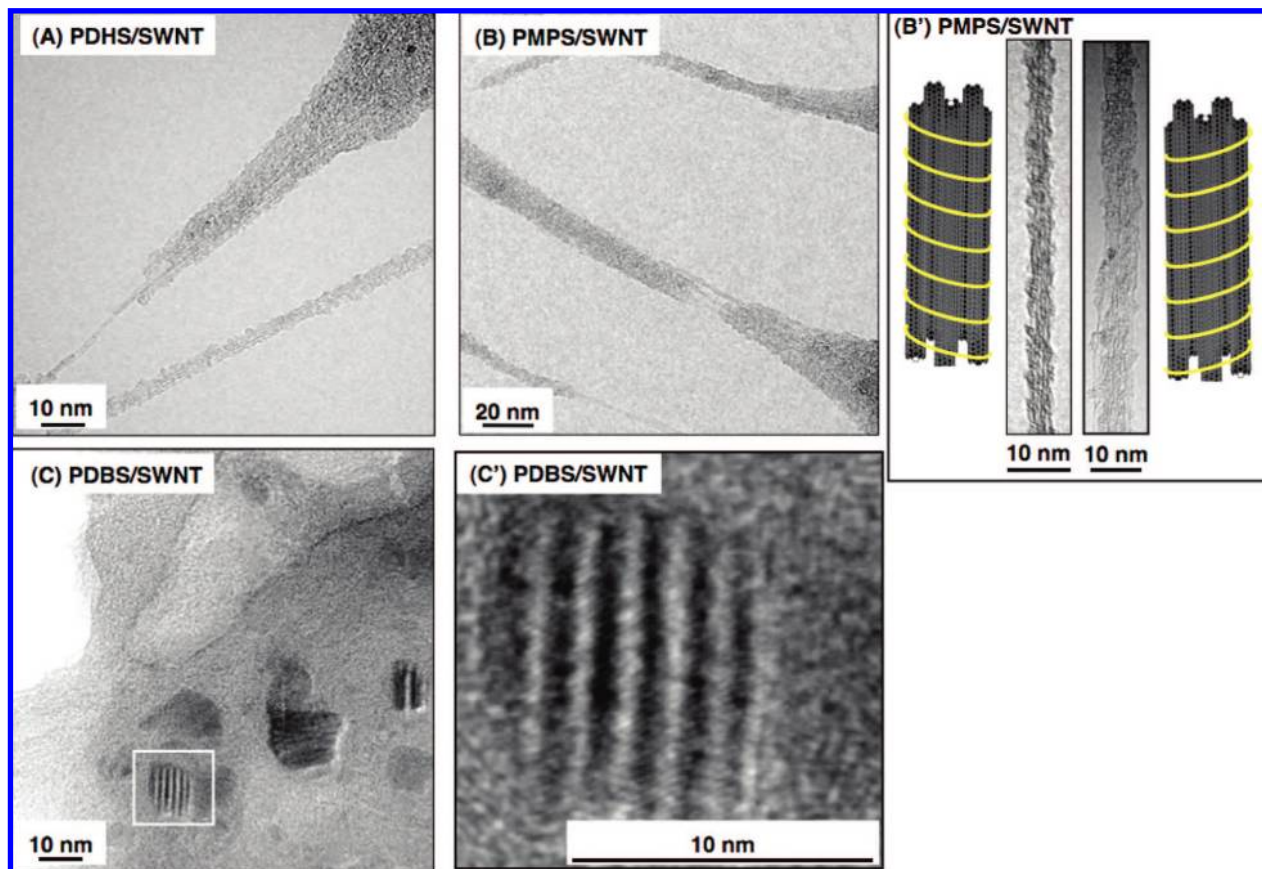


**Figure 2.** TEM images of the mixtures of SWNTs and PSi's prepared by HSV. (A) PDHS/SWNT, (B) PMPS/SWNT, and (C) PDBS/SWNT. (B') enlarged images of SWNT bundles helically wrapped by PMPS with both *P*- and *M*-screw senses. (C') enlarged image of the square in (C). All samples were cast on a microgrid and then dried under a gentle stream of  $N_2$  gas.

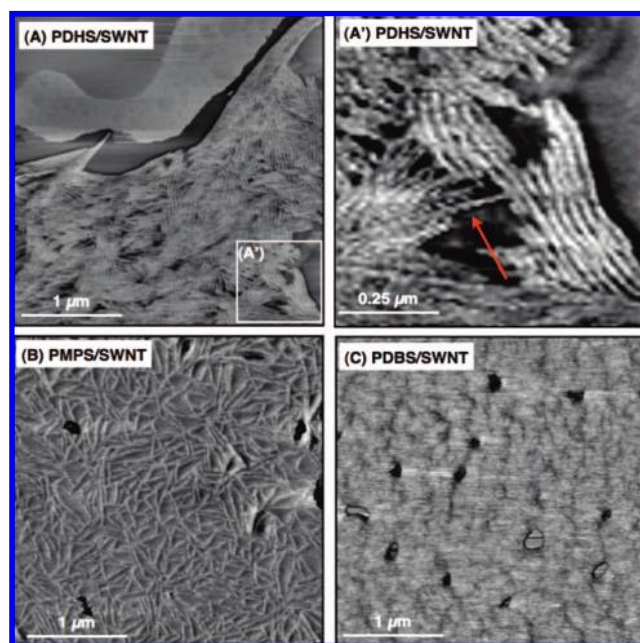


**Figure 3.** AFM images of (A) PDHS/SWNT, (B) PMPS/SWNT, and (C) PDBS/SWNT. (A') Enlarged image of the square in (A). Samples were cast on a freshly cleaved mica (001) surface and then dried under a gentle stream of  $N_2$  gas.

diameters of each chain were measured to be  $\sim 1.8$  nm, which was in agreement with the PDBS diameter calculated from the

CPK model ( $\sim 2$  nm) (Figure 2C').<sup>46</sup> On the basis of the fact that an optically active PSi with a semiflexible main chain spontaneously adopts an ordered liquid crystalline phase,<sup>47</sup> PDBS, the optically "inactive" PSi with a semiflexible main chain, may also prefer the liquid crystalline-like domains rather than wrapping around the SWNTs. Here we were led to the clear conclusion that the stiffness of PSi's greatly affects their wrapping behavior onto the cylindrical SWNT surfaces. As expected from the DSC results, both flexible PDHS and random-coiled PMPS helped to debundle the pristine SWNTs and simultaneously wrapped helically around the SWNTs through HSV. However, the semiflexible PDBS hardly debundled the pristine SWNTs, even after the same HSV procedure, probably because the semiflexible PDBS itself preferentially formed thermodynamically stable liquid crystalline domains rather than wrapping onto the SWNT at the expense of a gain in enthalpy.

Further AFM observations revealed that subtle changes in the main chain stiffness of the PSi's led to noticeably different morphologies on an atomically flat mica (001) surface. The isooctane solutions of PSi/SWNT were cast on freshly cleaved mica (001) and dried under a gentle stream of  $N_2$  gas. AFM observations were carried out with a phase mode (Nanoscope III, Digital Instruments, Santa Barbara, CA).<sup>48</sup> In the PDHS/SWNT cast film, almost uniform fibers with a 1.6 nm diameter and a length of several  $\mu\text{m}$  were observed (Figure 3A).

(46) Kawabe, T.; Naito, M.; Fujiki, M. *Macromolecules* **2008**, *41*, 1952–1960.

(47) Okoshi, K.; Kamee, H.; Suzaki, G.; Tokita, M.; Fujiki, M.; Watanabe, J. *Macromolecules* **2002**, *35*, 4556–4559.

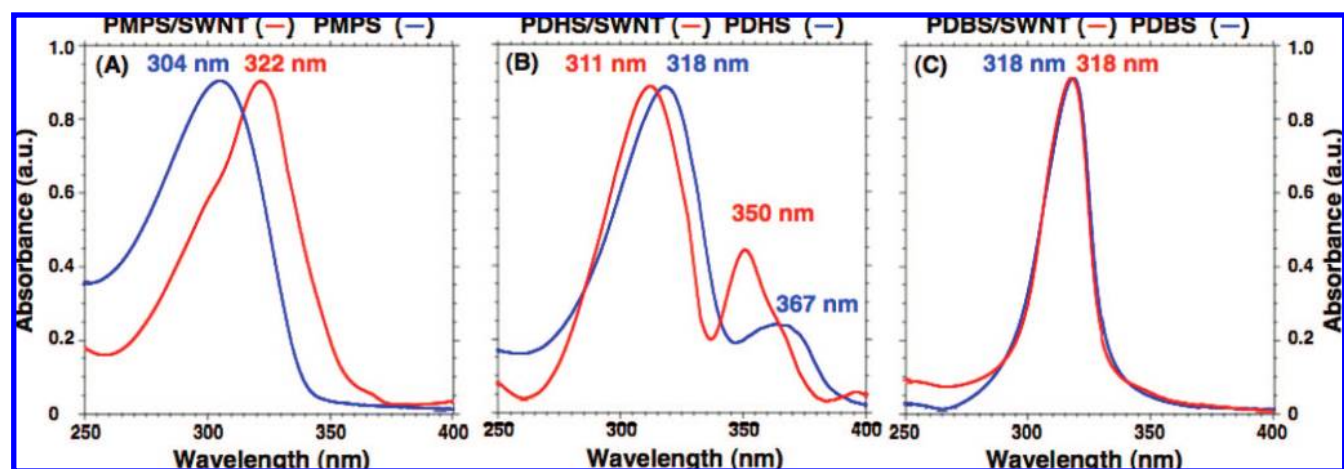


**Figure 4.** UV spectra of PSi and PSi/SWNT complex on quartz. (A) PMPS (blue) and PMPS/SWNT (red), (B) PDHS (blue) and PDHS/SWNT (red), and (C) PDBS (blue) and PDBS/SWNT (red). PSi/SWNT complexes were prepared with HSVM. All samples were cast on quartz substrates.

Furthermore, the PDHS-wrapped SWNTs spontaneously assembled to form horizontally aligned single layers during an evaporation of a good solvent for PDHS, isooctane. Moreover, the fibers spontaneously aligned in certain directions. Considering the length and diameter of PDHS ( $\sim 1.7$  nm in a diameter,  $d$ ) and CoMoCAT-SWNTs ( $>$ several  $\mu\text{m}$  in  $l$ ,  $0.8$  nm in  $d$ ), the fibrous structures seem to correspond to the individual and nonaggregated PDHS-wrapped SWNT chains. Furthermore, from the enlarged AFM image of Figure 3A, we found that PDHS wrapping on the SWNT single chains were in helical structures, as seen in the TEM image of PMPS/SWNT (see the orange arrow in Figure 3A). Note that we could not observe such noticeable structures, but randomly dispersed bundles from the pristine SWNTs treated with HSVM with the exact same procedure (see Figure S1 in the Supporting Information). The PMPS/SWNTs displayed extensively developed network structures, which consisted of straight rods with an average diameter of  $1.2$ – $1.8$  nm (Figure 3B). We have reported that when the random-coiled PMPS are immobilized onto the atomically flat mica (001) surface, the PMPS form dome-like structures, reflecting their flexible features.<sup>49</sup> Therefore, the straight rods were reasonably concluded to be the PMPS-wrapped SWNTs. In addition, we have also reported that the SWNTs with a length below  $\sim 1$   $\mu\text{m}$  align  $120^\circ$  to one another along directions of the mica surface and are mutually connected when the SWNTs form complexes with 8-quinolinol metal chelate derivatives through HSVM.<sup>37</sup> Therefore, the network structures formed by the shorter SWNTs ( $< 1$   $\mu\text{m}$ ) would be an inherent surface behavior of the complexes with the SWNTs and the solubilizing agents. In contrast, the PDBS/SWNT cast film did not form any noticeable structures, but a rugged thin film, which seems to support that no complexation with SWNTs occurred as a result of HSVM, as expected from the DSC and TEM results (Figure 3C).

Finally, the relationship between the conformation of the PSi's and their wrapping behaviors was further elucidated using ordinary UV spectroscopy. UV absorption bands derived from  $\text{Si}\sigma$ – $\text{Si}\sigma^*$  transitions of both PDHS and PMPS at  $300$ – $380$  nm changed drastically during HSVM, indicating that their con-

formations changed during wrapping onto the SWNTs, whereas that of the semiflexible PDBS remained unchanged. Figure 4 shows UV absorption spectra of cast films of PSi's and PSi/SWNTs. In the case of the PMPS cast film, the UV absorption band of PMPS appeared at  $304$  nm. Because the PMPS-wrapped SWNTs were generated with HSVM, the  $304$  nm UV absorption band was red-shifted to  $322$  nm. Here, the  $304$  and  $322$  nm UV absorption bands originated from PMPS with dihedral angles of ca.  $140$  and  $166^\circ$ , respectively.<sup>50</sup> Therefore, these significant red-shifts in the UV absorption bands indicate that the PMPS molecules changed their helical pitches and became looser during wrapping onto the SWNTs. Furthermore, PDHS demonstrated additional complicated spectral changes. PDHS cast film originally exhibited two absorption bands at  $318$  and  $367$  nm, which were assigned deviant ( $\phi$ :  $\sim 151^\circ$ ) and anti ( $\phi$ :  $\sim 180^\circ$ ), respectively.<sup>50</sup> After wrapping onto the SWNTs with HSVM, the  $367$  nm UV absorption band blue-shifted to  $350$  nm, and its absorption intensity nearly doubled, whereas the  $318$  nm UV absorption band slightly blue-shifted by only  $7$  nm. Here, the  $350$  nm band is assigned to PDHS with a dihedral angle of  $175^\circ$ .<sup>50</sup> With the results from the DSC, AFM, and TEM experiments, the changes in the conformation of PDHS after wrapping onto the SWNTs was reasonably described as follows: PDHS in a cast film adopts both crystalline and disordered phases with main chain conformations of anti and deviant, respectively.<sup>51</sup> When the PDHS solid was mechanochemically mixed with the pristine SWNTs, the crystalline alkyl side chains of PDHS were disordered during wrapping onto the SWNTs, with the PDHS dihedral angle decreasing from  $180^\circ$  to  $175^\circ$ . The changes in the dihedral angles of the PMPS and PDHS during wrapping appear to be induced by the curvatures of the cylindrical SWNT surfaces, hereinafter described in detail. However, PDBS exhibited an intense UV absorption band at around  $318$  nm with a relatively narrow fwhm of  $2075$   $\text{cm}^{-1}$ , indicating that semiflexible PDBS adopts a  $7_3$  helix structure with a dihedral angle  $\sim 154^\circ$ . The  $318$  nm UV absorption band of PDBS remained unchanged after HSVM, suggesting that the conformation of PDBS was not affected by the HSVM. It is noteworthy that such conformational changes were not observed

(48) Diameters of the PSi/SWNTs were estimated from the cross-section analyses of their topographic images. (See, Figure S2 in the Supporting Information).

(49) Naito, M.; Saeki, N.; Fujiki, M.; Ohira, A. *Macromolecules* **2007**, *40*, 648–652.

(50) Sasanuma, Y.; Kato, H.; Kaito, A. *J. Phys. Chem. B* **2003**, *107*, 11852–11860.

(51) Frank, C. W.; Rao, V.; Despotopoulou, M. M.; Pease, R. F. W.; Hinsberg, W. D.; Miller, R. D.; Rabolt, J. F. *Science* **1996**, *273*, 912–915.

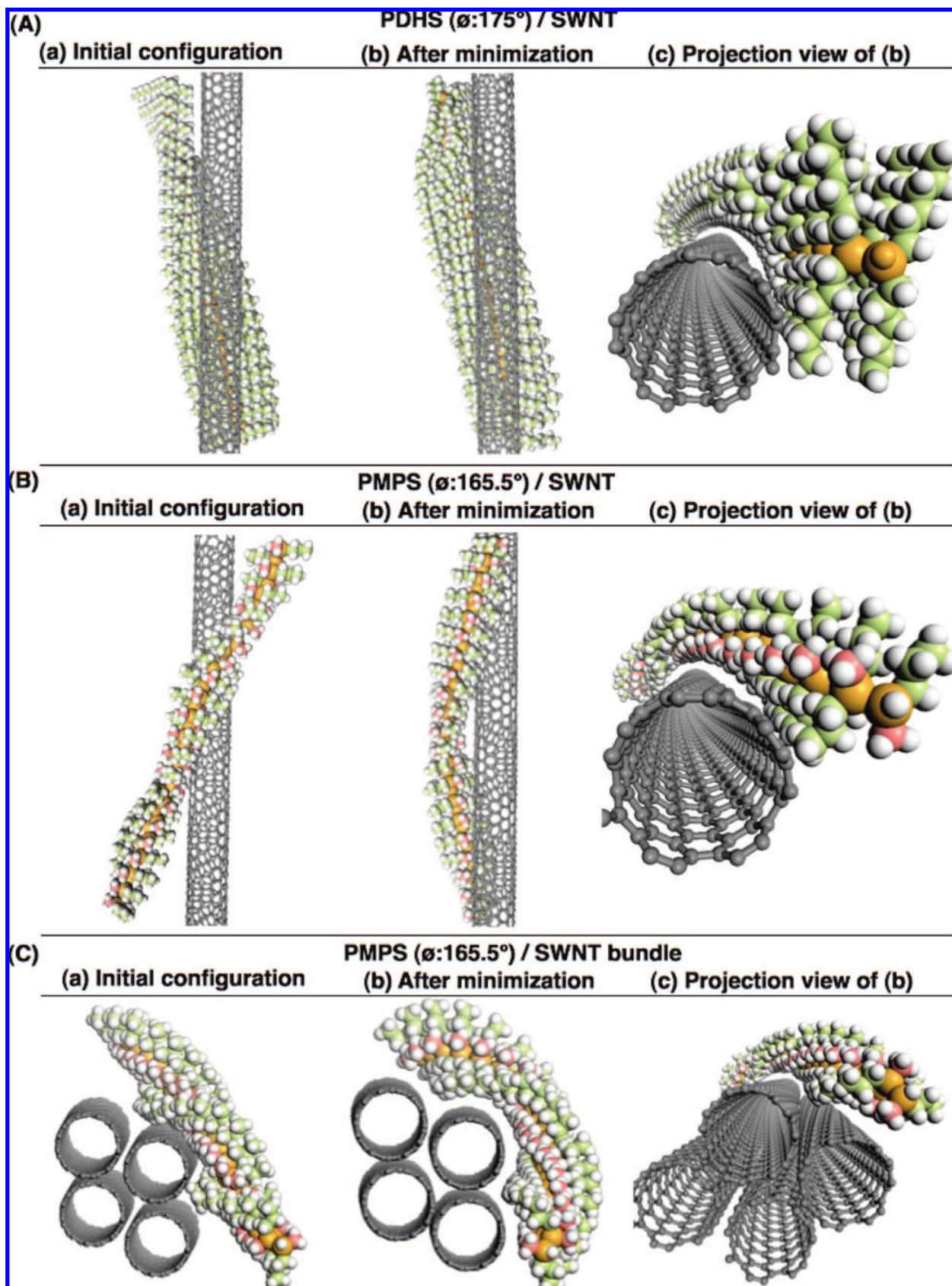


**Figure 5.** Proposed structures of PSi/SWNT complexes. (A) PDHS/SWNT single chain, (B) PMPS/SWNT single chain, and (C) PMPS/SWNT bundle. To simplify the calculation, PSi oligomer with 40 monomers (with 40-Si repeating units) and SWNTs (7,5) were employed as a model of PSi's and CoMoCAT SWNTs, respectively. SWNT bundle was consisted of 4-SWNTs (7,5). PCFF was used as a force field.

when mixtures of PSi/SWNT were prepared by sonication, probably because the sonication could not sufficiently debundle

the pristine SWNTs or the main chains of PSi's were sheared during the sonication process.

To further clarify the nature of the conformation-dependent polymer wrapping behavior of SWNTs with PSi's, computational studies with molecular mechanics calculations were performed using PCFF force fields (Materials Studio 4.0, Accelrys Inc., San Diego, CA). To simplify the calculations, PSi oligomers with 40-Si repeating units and SWNTs with the chiral vector (7,5) (diameter: 8.17 Å, length: 88.95 Å) were employed as models of PSi's and SWNTs, respectively. First, the most stable structures of the PSi's alone were optimized, in which the dihedral angles were constrained to certain degrees estimated from the values of  $\lambda_{\max}$  by the UV absorption results; thus,  $\phi_{\text{PDBS}}$ : 154°,  $\phi_{\text{PMPS}}$ : 140° and 166°, and  $\phi_{\text{PDHS}}$ : 151° and 175° were set as the dihedral angles. Here the apparent features of PSi's after the calculation could be classified into two categories, that is, the groups with or without wrapping ability. Thus, the SWNT-wrappable PSi's, such as PDHS with  $\phi$  of 175° or PMPS with  $\phi$  of 166°, possessed the helical grooves formed by the alkyl side chains along with the helical Si main chain [see, Figure S3(a) in the Supporting Information]. The others, without the ability to wrap onto the SWNTs, also adopted helical conformations, although the significant difference is that their alkyl side chains were distributed equally to surround the Si main chains without forming the grooves [see, Figure S3(b) in the Supporting Information]. As such, it was clearly demonstrated that the relationship between the alkyl-side-chain-formed helical grooves and the diameters of the SWNTs could dictate the eventual wrapping behaviors of the PSi's onto the SWNTs. Thus, for the SWNT-wrappable PSi's, such as PDHS with  $\phi$  of 175° or PMPS with  $\phi$  of 166°, the SWNTs (7,5) were positioned along the helical grooves of the preoptimized PSi's, as an initial configuration for the calculation of the complex between the PSi's and SWNTs, and then the potential energy minima of the PSi-SWNT complexes was further optimized with no constraints on any configurations [Figure 5, parts A(a) and B(a)]. It is immediately noticeable that interaction between PSi's and SWNTs substantially changes the conformation of the flexible PDHS and random-coiled PMPS to fit onto the curvatures of the SWNT (7,5) surface [Figure 5, parts A(b) and B(b)]. From the projection views of the complexes, it is apparent that the alkyl side chains are bound to the cylindrical substrate provided by the SWNTs [Figure 5, parts A(c) and B(c)]. This indicates that the wrapping behavior of PSi's onto SWNTs may be induced primarily by the CH- $\pi$  interaction between alkyl side chains of PSi's and SWNTs, not the  $\sigma$ - $\pi$  interaction between the Si main chain of the PSi's and the SWNTs. To estimate the degrees of the binding energy of the CH- $\pi$  interaction between alkyl side chains and SWNTs, FT-IR spectroscopy was conducted (see Figure S5 in the Supporting Information). Comparing the IR absorption bands of the stretching vibration modes of the methyl (CH<sub>3</sub>-) and methylene (CH<sub>2</sub>-) groups in the region from 2800 to 3100 cm<sup>-1</sup> between PSi's and PSi/SWNT complexes, no significant changes were detected. This result indicates that each the CH- $\pi$  interactions between the single alkyl side chains of PSi's and the SWNTs is negligibly small in the PSi's wrapped onto the SWNTs, although it may become an essentially important driving force when such subtle binding energy is cooperatively amplified along the Si main chains. We also considered the effect of diastereoisomeric complexes between the SWNTs and PSi's. However, a significant difference was not observed due to the relatively small binding energy of the CH- $\pi$  interaction. To address the situation, more appropriate force fields would be required.

In TEM observations (Figure 2, parts A and B), we have mentioned that random-coiled PMPS and flexible PDHS could effectively wrap around not only single chains of SWNTs, but also small bundles of the SWNTs. Here, a key question has arisen whether the diameter of a single SWNT (0.8 nm) is directly correlated with the conformation of the PSi chain optimized by the simulation because the observed apparent diameters of the SWNT bundles (1–20 nm) are expected to be much greater than that of a single SWNT. To address the question, the molecular mechanics calculation of the wrapping of random-coiled PSi, PMPS, was further carried out on a small SWNT bundle. Figure 5(C) shows an optimized complex of PMPS and a SWNT bundle. As seen in the case of the SWNT single chain, the small SWNT bundle was successfully bound by PMPS. This result indicates that for PSi's wrapping around small SWNT bundles, the surface curvature of a single SWNT chain on the top surface of the SWNT bundles is essential, not the apparent diameters of the SWNT bundles.

## Conclusion

In summary, the results described in this study show, for the first time, how stiffness and conformation affect the wrapping behavior of chain-like polymers around SWNTs. Thus, random-coiled PMPS and flexible PDHS were successfully wrapped onto CoMoCAT-SWNTs, and their conformations were changed to fit the surface curvatures of the SWNTs. In contrast, semiflexible PDHS could not form the complex with SWNTs, and its conformation remained unchanged even after the same HSVM process. It was also revealed that the relationship between the initial conformations of the PSi's and the surface curvatures of SWNTs strongly affects the eventual wrapping behavior. Thus, when the SWNTs could be positioned along the helical grooves provided by the alkyl side chains of PSi's, the PSi's spontaneously wrapped onto the SWNT surface, induced by subtle but sufficiently strong CH- $\pi$  interactions between the alkyl side chains of PSi's and the SWNT surface. These results may be profitably used as a guide toward designing the type of chain-like polymers and conditions necessary to successfully wrap SWNTs with a particular range of diameters. The polymer wrapping behaviors of PSi's predicated on the diameter of CNTs will be presented in a forthcoming paper.

**Acknowledgment.** The authors thank Ms. Rie Nakashima and Mr. Shohei Katao for TEM observations. M.N. thanks Mr. Steven Nishida for reading the entire text in its original form. M.N. thanks Prof. Mikio Kataoka, Prof. Tsuyoshi Kawai, Prof. Kotohiro Nomura, and Dr. Kitiyanan Boonyarach for fruitful discussions. This work was partially supported by Grant-in-Aid for Young Scientists (B) (20750094) and for Scientific Research in Priority Areas (17067012) from the Ministry of Education, Culture, Sports Science, and Technology, MEXT, Japan, JST in Research for Promoting Technological Seeds (10-073), Nara Institute of Science and Technology, and Kinki Invention Center.

**Supporting Information Available:** Detailed procedures, including Topographic AFM images, FT-IR, and optimized structures of the PSi's with a MM calculation using PCFF as a force field. This material is available free of charge via the Internet at <http://pubs.acs.org>.

JA806109Z